Collision Cross Sections of Proteins and Their Complexes: A Calibration Framework and Database for Gas-Phase Structural Biology

ARTICLE *in* ANALYTICAL CHEMISTRY · OCTOBER 2010

Impact Factor: 5.64 · DOI: 10.1021/ac1022953 · Source: PubMed

6 AUTHORS, INCLUDING:

Zoe Hall
University of Cambridge
14 PUBLICATIONS **567** CITATIONS
SEE PROFILE

Kevin Giles
Waters Corporation
49 PUBLICATIONS **2,857** CITATIONS
SEE PROFILE

John Brian Hoyes
Waters Corporation
19 PUBLICATIONS **1,146** CITATIONS
SEE PROFILE

Carol V Robinson
University of Oxford
432 PUBLICATIONS **22,885** CITATIONS
SEE PROFILE

Anal. Chem. **2010,** *82,* 9557–9565

Collision Cross Sections of Proteins and Their Complexes: A Calibration Framework and Database for Gas-Phase Structural Biology

Matthew F. Bush,[†] Zoe Hall,[†] Kevin Giles,[‡] John Hoyes,[‡] Carol V. Robinson,*[,†] and Brandon T. Ruotolo*[,§]

Department of Chemistry, Physical and Theoretical Chemistry Laboratory, University of Oxford, South Parks Road, Oxford OX1 3QZ, United Kingdom, Waters Corporation, Floats Road, Wythenshawe, Manchester M23 9LZ, United Kingdom, and Department of Chemistry, University of Michigan, Ann Arbor, Michigan 48109, United States

Collision cross sections in both helium and nitrogen gases were measured directly using a drift cell with RF ion confinement inserted within a quadrupole/ion mobility/time-of-flight hybrid mass spectrometer (Waters Synapt HDMS, Manchester, U.K.). Collision cross sections for a large set of denatured peptide, denatured protein, native-like protein, and native-like protein complex ions are reported here, forming a database of collision cross sections that spans over 2 orders of magnitude. The average effective density of the native-like ions is 0.6 g cm^{-3}, which is significantly lower than that for the solvent-excluded regions of proteins and suggests that these ions can retain significant memory of their solution-phase structures rather than collapse to globular structures. Because the measurements are acquired using an instrument that mimics the geometry of the commercial Synapt HDMS instrument, this database enables the determination of highly accurate collision cross sections from traveling-wave ion mobility data through the use of calibration standards with similar masses and mobilities. Errors in traveling-wave collision cross sections determined for native-like protein complexes calibrated using other native-like protein complexes are significantly less than those calibrated using denatured proteins. This database indicates that collision cross sections in both helium and nitrogen gases can be well-correlated for larger biomolecular ions, but non-correlated differences for smaller ions can be more significant. These results enable the generation of more accurate three-dimensional models of protein and other biomolecular complexes using gas-phase structural biology techniques.

Ion mobility mass spectrometry (IM-MS) can provide detailed insights into the structures of macromolecules and macromolecular complexes, including those that are most challenging for condensed-phase techniques.[1] IM-MS data for Aβ oligomers[2] and β_2-microglobulin oligomers[3] reveal detailed insights into the size distributions and shapes associated with the initial self-assembly of these amyloid-forming peptides. Collision cross sections (Ω), which depend strongly on ion shape and can be determined using IM-MS experiments, for "subcomplexes" generated from large biomolecular complexes have been used to obtain geometric restraints between several subunit proteins comprising the human eukaryotic initiation factor 3,[4,5] a large complex with 13 unique protein subunits for which there is no high-resolution structure. Mobility measurements suggest that a distribution of several apo-myoglobin proteins can be trapped by the 20S proteasome,[6] and the Ω values and average charge states measured for GroEL and several GroEL:client complexes exhibit similarities suggesting that the clients remain encapsulated within the complexes after introduction to the gas phase.[7] Based on these and other successes, there is considerable interest in applying IM-MS techniques to obtain detailed insights into ever-more-challenging biological targets, including complexes with greater mass and heterogeneity.

Applications of IM-MS have increased dramatically since the introduction of commercial quadrupole/traveling-wave ion mobility/time-of-flight hybrid mass spectrometers,[8] which have enabled the use of IM-MS by a user base with rapidly accelerating growth. Although the transport of ions through drift tubes with weak,

* To whom correspondence should be addressed. E-mail: carol.robinson@chem.ox.ac.uk (C.V.R.), bruotolo@umich.edu (B.T.R.).

[†] University of Oxford.

[‡] Waters Corporation.

[§] University of Michigan.

(1) Uetrecht, C.; Rose, R. J.; van Duijn, E.; Lorenzen, K.; Heck, A. J. R. *Chem. Soc. Rev.* **2010**, *39*, 1633–1655.

(2) Bernstein, S. L.; Dupuis, N. F.; Lazo, N. D.; Wyttenbach, T.; Condron, M. M.; Bitan, G.; Teplow, D. B.; Shea, J. E.; Ruotolo, B. T.; Robinson, C. V.; Bowers, M. T. *Nat. Chem.* **2009**, *1*, 326–331.

(3) Smith, D. P.; Radford, S. E.; Ashcroft, A. E. *Proc. Natl. Acad. Sci. U.S.A.* **2010**, *107*, 6794–6798.

(4) Leary, J. A.; Schenauer, M. R.; Stefanescu, R.; Andaya, A.; Ruotolo, B. T.; Robinson, C. V.; Thalassinos, K.; Scrivens, J. H.; Sokabe, M.; Hershey, J. W. B. *J. Am. Soc. Mass Spectrom.* **2009**, *20*, 1699–1706.

(5) Pukala, T. L.; Ruotolo, B. T.; Zhou, M.; Politis, A.; Stefanescu, R.; Leary, J. A.; Robinson, C. V. *Structure* **2009**, *17*, 1235–1243.

(6) Loo, J. A.; Berhane, B.; Kaddis, C. S.; Wooding, K. M.; Xie, Y. M.; Kaufman, S. L.; Chernushevich, I. V. *J. Am. Soc. Mass Spectrom.* **2005**, *16*, 998–1008.

(7) van Duijn, E.; Barendregt, A.; Synowsky, S.; Versluis, C.; Heck, A. J. R. *J. Am. Chem. Soc.* **2009**, *131*, 1452–1459.

(8) Pringle, S. D.; Giles, K.; Wildgoose, J. L.; Williams, J. P.; Slade, S. E.; Thalassinos, K.; Bateman, R. H.; Bowers, M. T.; Scrivens, J. H. *Int. J. Mass Spectrom.* **2007**, *261*, 1–12.

10.1021/ac1022953
Published on Web 10/27/2010

uniform electric fields is well-understood and characterized,[9−12] the transport of ions through ion mobility cells with traveling waves is less well-understood. Ω values for ions transported by traveling waves are typically determined by calibrating drift times for ions of interest against those measured for ions of known Ω values.[13−15] One challenge is that absolute Ω values in the literature[16−20] that could be used for calibration have significantly higher mobilities and lower masses than the macromolecular complexes of greatest interest, which can result in significant extrapolation errors.[21]

Most reported Ω values for protein complexes have been based on calibration using denatured monomeric proteins[7,15,22,23] whose Ω values in helium gas (Ω_{He}) have been reported, typically ubiquitin, cytochrome *c*, and myoglobin. There is great interest in using protein complex standards to calibrate traveling-wave drift times for protein complexes of interest, which should reduce extrapolation errors. For example, Ω values for several protein complexes and subcomplexes[5] have been determined based on calibration using both denatured monomeric proteins, previously characterized in drift-tube experiments,[16−18] and selected protein complexes, characterized using traveling-wave experiments in which drift times were measured using the minimum wave height that resulted in ion transmission along a single wavefront ("surfing the wave") on a modified Synapt high-definition mass spectrometry (HDMS) instrument.[24] In these cases,[7,15,22,23] drift times for the protein complex ions of interest and the calibrant ions were measured in nitrogen gas, but were calibrated using Ω_{He} values for the calibrant ions to yield calibrated Ω_{He} values for the analytes. This is desirable to enable access to the comparatively large quantity of Ω_{He} values in the literature and the availability of computational tools for estimating the Ω_{He} values for structural models.[25,26] However, the correlation between Ω_{He} and Ω_{N_2} has not been thoroughly characterized.

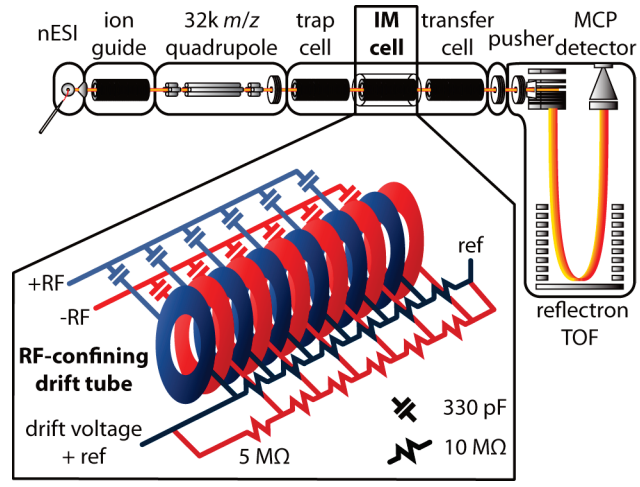

Figure 1. Modified quadrupole/ion mobility/time-of-flight hybrid mass spectrometer used for absolute Ω measurements. The ion mobility cell in this instrument has a linear voltage gradient along the axis of ion transmission and RF confinement in the radial direction (RF-confining drift tube). The voltage gradient is established by a pair of voltage divider networks consisting of 10 MΩ resistors (plus one 5 MΩ resistor, labeled, to correctly offset networks). In contrast to the standard Synapt HDMS, traveling waves are not used in this ion mobility cell.

Here, we report Ω measurements in both helium and nitrogen gases for a large set of biomolecular ions, including denatured peptide, denatured protein, native-like protein, and native-like protein complex ions. Ω values in these experiments are determined directly from drift times measured in a low-pressure (~2 Torr) drift tube with radio-frequency (RF) confinement, without the need for mobility calibration. These ions have masses ranging from 0.5 to 800 kDa and Ω values ranging from 1 to >200 nm^2 and thus are ideal for calibrating IM-MS results for a wide range of ions of interest. Access to this information also enables the precise quantification of the errors associated with traveling-wave Ω measurements of large biomolecular ions. We then use this new database and error analysis to propose a set of best practices for Ω calibration using the values reported herein. These results enable the generation of more accurate three-dimensional models of protein and other biomolecular complexes using gas-phase structural biology techniques.

EXPERIMENTAL METHODS

Measurements of absolute collision cross sections (Ω) were performed on a modified Synapt G1 HDMS (Waters Co., Manchester, U.K.) instrument[8] in which the traveling-wave ion mobility cell was replaced by an 18-cm drift cell that has a radial RF ion confinement (radio frequency of 2.7 MHz and peak-to-peak amplitude of 200 V) and a linear voltage gradient to direct ions along the axis of transmission to the time-of-flight mass analyzer (Figure 1). This cell uses no traveling waves, but was fabricated in much the same way as the traveling-wave ion mobility cell used

(9) Mason, E. A.; McDaniel, E. W. *Transport Properties of Ions in Gases*; Wiley: New York, 1998.
(10) Wyttenbach, T.; Bowers, M. T. *Mod. Mass Spectrom.* **2003**, *225*, 207–232.
(11) Bohrer, B. C.; Mererbloom, S. I.; Koeniger, S. L.; Hilderbrand, A. E.; Clemmer, D. E. *Annu. Rev. Anal. Chem.* **2008**, *1*, 293–327.
(12) Kanu, A. B.; Dwivedi, P.; Tam, M.; Matz, L.; Hill, H. H. *J. Mass Spectrom.* **2008**, *43*, 1–22.
(13) Ruotolo, B. T.; Benesch, J. L. P.; Sandercock, A. M.; Hyung, S. J.; Robinson, C. V. *Nat. Protoc.* **2008**, *3*, 1139–1152.
(14) Smith, D. P.; Knapman, T. W.; Campuzano, I.; Malham, R. W.; Berryman, J. T.; Radford, S. E.; Ashcroft, A. E. *Eur. J. Mass Spectrom.* **2009**, *15*, 113–130.
(15) Scarff, C. A.; Thalassinos, K.; Hilton, G. R.; Scrivens, J. H. *Rapid Commun. Mass Spectrom.* **2008**, *22*, 3297–3304.
(16) Valentine, S. J.; Counterman, A. E.; Clemmer, D. E. *J. Am. Soc. Mass Spectrom.* **1997**, *8*, 954–961.
(17) Shelimov, K. B.; Clemmer, D. E.; Hudgins, R. R.; Jarrold, M. F. *J. Am. Chem. Soc.* **1997**, *119*, 2240–2248.
(18) Clemmer, D. E. Cross Section Database, http://www.indiana.edu/~clemmer/Research/cross%20section%20database/cs%20database.htm (accessed Oct 18, 2010).
(19) Tao, L.; McLean, J. R.; McLean, J. A.; Russell, D. H. *J. Am. Soc. Mass Spectrom.* **2007**, *18*, 1232–1238.
(20) Valentine, S. J.; Counterman, A. E.; Clemmer, D. E. *J. Am. Soc. Mass Spectrom.* **1999**, *10*, 1188–1211.
(21) Shvartsburg, A. A.; Smith, R. D. *Anal. Chem.* **2008**, *80*, 9689–9699.
(22) Ruotolo, B. T.; Hyung, S. J.; Robinson, P. M.; Giles, K.; Bateman, R. H.; Robinson, C. V. *Angew. Chem., Int. Ed.* **2007**, *46*, 8001–8004.
(23) Ruotolo, B. T.; Giles, K.; Campuzano, I.; Sandercock, A. M.; Bateman, R. H.; Robinson, C. V. *Science* **2005**, *310*, 1658–1661.
(24) Giles, K.; Wildgoose, J. L.; Langridge, D. J.; Campuzano, I. *Int. J. Mass Spectrom.*, published online Oct 22, 2009, http://dx.doi.org/10.1016/j.ijms.2009.10.008.
(25) von Helden, G.; Hsu, M. T.; Kemper, P. R.; Bowers, M. T. *J. Chem. Phys.* **1991**, *95*, 3835–3837.
(26) Shvartsburg, A. A.; Jarrold, M. F. *Chem. Phys. Lett.* **1996**, *261*, 86–91.

in the standard instrument.[8,27] The drift cell consists of 122 gold-coated circular electrodes that have an internal diameter of 7 mm, are 0.5 mm thick, and have a center-to-center spacing of 1.5 mm. These electrodes are connected to printed circuit boards that have voltage divider networks composed of 10 MΩ surface-mount resistors. Potentials of the electrodes in this cell reduce in constant decrements from the entrance to exit electrodes; the difference in potentials between the entrance and exit electrodes will be referred to as the drift voltage. The cell is enclosed in a 185-mm housing composed of two printed circuit board side plates, aluminum top and bottom plates, and stainless-steel end plates with 1.0-mm orifices for ion transmission.

Ω values were determined directly from the slopes of drift time versus reciprocal drift voltage plots,[28] using drift voltages ranging from 50 to 200 V in 2−2.6 Torr of either helium or nitrogen gas. Typically, drift times were measured at 10 drift voltages, plotted as a function of reciprocal drift voltage,[28] and yielded R^2 correlation coefficients >0.9997. Pressures were measured using a calibrated absolute pressure transducer (MKS Baratron model 626A, Wilmington, MA) that was connected directly to the ion mobility cell. The amplitude of the RF in the drift tube was 200 V for all database measurements; arrival time distributions for tetrapropyl ammonium ions measured at 20, 50, 100, and 200 V RF amplitudes are indistinguishable, but signal intensities decrease substantially when low RF amplitudes are used. For species that yield intense signals, in particular, the denatured peptide and protein ions, ion beams were attenuated prior to the IM cell to minimize space-charge effects and detector saturation.

Arrival time distributions for single ion species reported here yielded resolutions of 15−20 ($t_D/\Delta t_D$, fwhm). These values are slightly greater than those reported in some traveling-wave ion mobility experiments on standard Synapt G1 instruments,[8,14,22] consistent with the use of higher mobility gas pressures[8] (enabled by smaller ion mobility cell apertures) and careful control of ion densities. The performance of the instrument as a mass analyzer, both with and without separation by ion mobility, is similar to that of a standard Synapt G1 HDMS instrument[8] equipped with a 32k m/z quadrupole mass filter.

All traveling-wave ion mobility experiments were performed on a standard Synapt G1 HDMS instrument equipped with a traveling-wave ion mobility cell containing 0.4 Torr of nitrogen gas and using methods reported previously.[13] Traveling-wave drift times were calibrated using a modified form of a protocol report previously.[13] Briefly, observed drift times (t_D) are corrected for m/z-dependent flight times

$$t_D' = t_D - c\sqrt{m/Z} \tag{1}$$

The constant c is determined empirically as described previously.[13] Literature Ω_{He} values are corrected for charge and reduced mass

$$\Omega' = \frac{\Omega_{literature}\sqrt{\mu}}{z} \tag{2}$$

An exponential factor (X) is determined from the slope of the plot of $\ln(\Omega')$ as a function of $\ln(t_D')$. Calibrated Ω_{He} values are determined by plotting literature Ω_{He} values as a function of the final corrected drift times (t_D'')

$$t_D'' = t_D'^{X}\left(\frac{z}{\sqrt{\mu}}\right) \tag{3}$$

Sample sources and preparation protocols are summarized in Table S1 (Supporting Information). Ions are formed by nanoelectrospray ionization using gold-coated borosilicate micropipets.[29] For native-like protein complexes, instrument conditions were optimized for high-m/z ions.[13,29,30] Ion activation conditions, which depend most strongly on the sample cone voltage, the injection voltage into the trap cell, and the injection voltage into the drift tube, were minimized to conditions near the threshold for ion transmission. For most native-like protein complexes investigated here, these values were typically 15, 5−10, and 20 V, respectively. Higher voltages were required to observe the highest-mass protein complexes.

RESULTS AND DISCUSSION

Measuring Ion Mobilities Using an RF-Confining Drift Tube. Drift times in these experiments were measured using a modified Synapt G1 HDMS instrument in which the traveling-wave ion mobility cell was replaced with an 18-cm drift cell that has a radial RF ion confinement and a linear voltage gradient to direct ions along the axis of ion transmission to the mass analyzer (Figure 1). Drift cell field energies for these experiments ranged from 1.0 to 5.5 V cm^{-1} Torr^{-1}, values that are significantly less than the low-field limit reported (20−45 V cm^{-1} Torr^{-1})[31] for a large set of peptide ions;[20] the low-field limit for native-like protein and protein complex ions is even greater.[9,31] Ions in this drift tube are not subjected to traveling waves. Drift times in these experiments depend on interactions between ions and drift-gas molecules in the presence of a weak uniform electric field, conditions that are well-described in the literature.[9−12] Briefly, ion velocities (v) are proportional to the electric field (E) and the mobility of the ion (K) under the conditions in the drift tube

$$v = KE \tag{4}$$

To enable direct comparison of mobility values determined over a range of experimental conditions, it is convenient to report reduced mobility values (K_0) that are corrected to standard pressure (p_0 = 760 Torr) and temperature (T_0 = 273.15 K)

$$K_0 = \frac{pT_0}{p_0T}K \tag{5}$$

Representative data for denatured peptide, denatured protein, and native-like protein complex ions are shown in Figure S1 (Supporting Information). Measured drift times (t_D) in these experiments depend on the mobility of the ion, the electric field,

(27) Giles, K.; Pringle, S. D.; Worthington, K. R.; Little, D.; Wildgoose, J. L.; Bateman, R. H. *Rapid Commun. Mass Spectrom.* **2004**, *18*, 2401–2414.

(28) Kemper, P. R.; Dupuis, N. F.; Bowers, M. T. *Int. J. Mass Spectrom.* **2009**, *287*, 46–57.

(29) Hernandez, H.; Robinson, C. V. *Nat. Protoc.* **2007**, *2*, 715–726.

(30) Benesch, J. L. P.; Ruotolo, B. T.; Simmons, D. A.; Robinson, C. V. *Chem. Rev.* **2007**, *107*, 3544–3567.

(31) Verbeck, G. F.; Ruotolo, B. T.; Gillig, K. J.; Russell, D. H. *J. Am. Soc. Mass Spectrom.* **2004**, *15*, 1320–1324.

and the transport time of ions from the exit of the drift region to the time-of-flight mass analyzer (t_0)

$$t_D = \frac{\text{length}}{KE} + t_0 \quad (6)$$

For the experiments in Figure S1 (Supporting Information), drift times were measured at 10 drift voltages, ranging from 60 to 200 V, in 2.0 Torr of nitrogen gas. Linear regressions of the data result in R^2 values of 0.9997−0.9999, indicating that any higher-order effects on drift times are very small. However, drift times measured at very low drift voltages exhibit a slight deviation toward longer drift times. These effects increase with decreasing drift voltage, but no statistical evidence for these effects has been observed for data obtained at drift voltages ≥50 V. Note that somewhat analogous effects have been observed in ion funnels following drift tubes.[28] The slopes of the best fit lines in Figure S1 (Supporting Information), and the corresponding mobility values, have relative errors <0.6%.

In many ion mobility experiments, the intercepts of the best fit lines (t_0) exhibit large m/z dependencies that are attributable to a time-of-flight separation in the ion optics prior to the mass analyzer. In contrast, t_0 values in Figure S1 of the Supporting Information (0.55−0.75 ms) depend less on m/z because ion velocities in the transfer cell after the drift tube are expected to be very close to the velocity of the traveling wave used to transport ions in that cell (200 m/s for experiments in Figure S1, Supporting Information).[13,27] The small differences in observed t_0 values are consistent with a small time-of-flight separation after the transfer cell but before the ions are introduced to the time-of-flight mass analyzer.

Collision Cross Sections. Mobilities in helium and nitrogen gases were measured for a wide range of peptide, protein, and protein complex ions. Ion species that were selected for inclusion in this study are all from samples that are commercially available, have facile preparation requirements (Table S1, Supporting Information), and yield stable ion currents using nanoelectrospray ionization. The charge states reported in Tables S2 and S3 (Supporting Information) are readily achieved using nanoelectrospray from the respective solutions and have single arrival time distributions (or one predominant distribution) under the gentle (minimal activation) conditions used in these experiments. Gentle experimental conditions, near the threshold for ion transmission, are desirable for these experiments to mitigate the effects of structural collapse, structural unfolding, and other structural transitions that have been observed for native-like protein complex ions that have been activated in the gas phase.[22,23,32,33]

The collision cross section (Ω) of an ion is related to its mobility through the Mason−Schamp equation[9−12]

$$\Omega = \frac{3e}{16N}\sqrt{\frac{2\pi}{\mu k_B T}}\frac{1}{K} \quad (7)$$

where N is the drift-gas number density, μ is the reduced mass of the ion and drift gas, k_B is the Boltzmann constant, and T is the drift-gas temperature. Recently, it has been suggested that the mobilities of biomolecular ions can be affected significantly by the inelasticity of collisions with drift-gas molecules, which would result in a smaller Ω value for a given mobility.[34] Pending further investigation, readers are welcome to adjust the Ω values reported here using the Millikan formula and assuming a correction factor of their choice.[34−36]

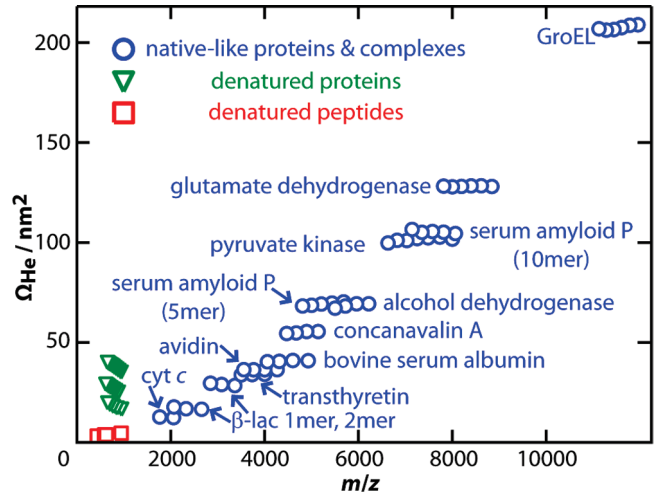

Figure 2. Collision cross sections in helium gas for the observed charge states of denatured peptide, denatured protein, native-like protein, and native-like protein complex ions as a function of m/z. Values in both helium and nitrogen gases are reported in Tables S2 and S3 of the Supporting Information.

Ω values are reported in Tables S2 and S3 (Supporting Information), and results in helium gas are also shown in Figure 2. These Ω values are the averages of replicate measurements of mobility; most of these averages are the results of three mobility measurements, each made on separate days using 10 drift time measurements. Errors in the slopes of individual drift time versus reciprocal drift voltage plots are typically 0.5−1.0%, but the standard deviation of measurements performed over long periods of time can be slightly larger (typically 0.5−2%). Additional sources of error include pressures, which were measured using a calibrated absolute pressure transducer (manufacturer-reported accuracy 0.25%), and the temperature in the ion mobility cell, estimated as the average ambient laboratory temperature (293 K, error ≈ 0.5%). Therefore, the errors for the mobilities and Ω values in this database are estimated to be <3%.

Comparisons with Literature. These Ω_{He} measurements can be compared with many values in the literature. For the 16 denatured peptide and protein ions reported both in Table S2 (Supporting Information) and in a database obtained from traditional drift tube measurements (reported errors of 1%),[17,18] values here are (0.3 ± 1.4)% larger. There are relatively few reported Ω_{He} values for native-like protein complexes. For example, Ω_{He} values determined from traveling-wave drift times in nitrogen gas and calibration with denatured protein ions for tetrameric transthyretin ($z = 15$)[22] and tetradecameric GroEL (charge-state-averaged)[7] are 29 ± 2 and 244 ± 3 nm^2, respectively, whereas we measured values of 34.0 and 207 nm^2,

(32) Benesch, J. L. P. *J. Am. Soc. Mass Spectrom.* **2009**, *20*, 341–348.
(33) Freeke, J.; Robinson, C. V.; Ruotolo, B. T. *Int. J. Mass Spectrom.*, published online Aug 12, 2009, http://dx.doi.org/10.1016/j.ijms.2009.08.001.
(34) Hogan, C. J.; de la Mora, J. F. *J. Am. Soc. Mass Spectrom.* **2010**, in press.
(35) Ku, B. K.; de la Mora, J. F. *Aerosol Sci. Technol.* **2009**, *43*, 241–249.
(36) Kim, J. H.; Mulholland, G. W.; Kukuck, S. R.; Pui, D. Y. H. *J. Res. Natl. Inst. Stand. Technol.* **2005**, *110*, 31–54.

respectively, for these ions. Surfing-the-wave traveling-wave drift time measurements[24] indicate that the charge-state-averaged Ω_{He} values for tetrameric transthyretin, pentameric serum amyloid P, and decameric serum amyloid P are 31.5, 58.8, and 88.9 nm^2, respectively (estimated error of 5%),[5] whereas we measured values of 34.0, 69.2, and 105 nm^2, respectively, for these ions. Differences between the Ω_{He} values obtained here and those in the literature, which all used instrumentation with similar geometries but less direct means to determine Ω_{He}, illustrate the need for a unified framework for obtaining Ω values in different laboratories.

Electrophoretic mobilities for many protein complexes have been measured using gas-phase electrophoretic mobility macromolecular analysis (GEMMA) experiments, and those results suggest that the average effective density of the ions in those experiments is 0.58 ± 0.05 g cm^{-3}.[37] Electrophoretic mobilities, which are reported as the Millikan diameter of a charged sphere with the same electrophoretic mobility as the ion of interest,[37,38] are not directly comparable to Ω values, but an analogous effective density (D_{eff}) was calculated (see Supporting Information). For the native-like ions investigated here (Table S3, Supporting Information), this analysis yields an average D_{eff} value of 0.61 ± 0.07 g cm^{-3}, which is in excellent agreement with the D_{eff} value reported previously.[37] These values are significantly less than densities estimated for the solvent-excluded regions of proteins (>1.2 g cm^{-3}),[39,40] which indicates that these ions have not collapsed to globular structures. Additionally, results for these native-like ions are inconsistent with highly extended or denatured structures. Structures with significantly larger Ω values are observed when the ions are activated significantly prior to ion mobility analysis,[22,33] whereas these native-like structures are observed over a modest range of gentle instrumental conditions. These results suggest that electrospray ionization can produce ions with significant memory of their solution-phase structure, including cavities and other higher-ordered structural elements.

Effects of Mobility Gas Selection. Most traveling-wave ion mobility separations using Synapt HDMS instruments are performed using nitrogen gas, but Ω_{He} values are desirable to enable comparisons with the literature and calculated Ω values for structural models.[25,26] This is typically achieved by calibrating traveling-wave drift times in nitrogen gas using Ω_{He} values.[13−15] This has been justified because calibration should correct for many systematic differences between K_0^{He} and $K_0^{N_2}$. Moreover, non-correlated differences between K_0^{He} and $K_0^{N_2}$ should be less significant for large biomolecular complexes with low charge densities than for small ions with high charge densities.[41] However, there are relatively few ions for which both Ω_{He} and Ω_{N_2} values have been measured directly under similar experimental conditions. This has made it challenging to assess the errors associated with using drift times measured in nitrogen to estimate Ω_{He} values.

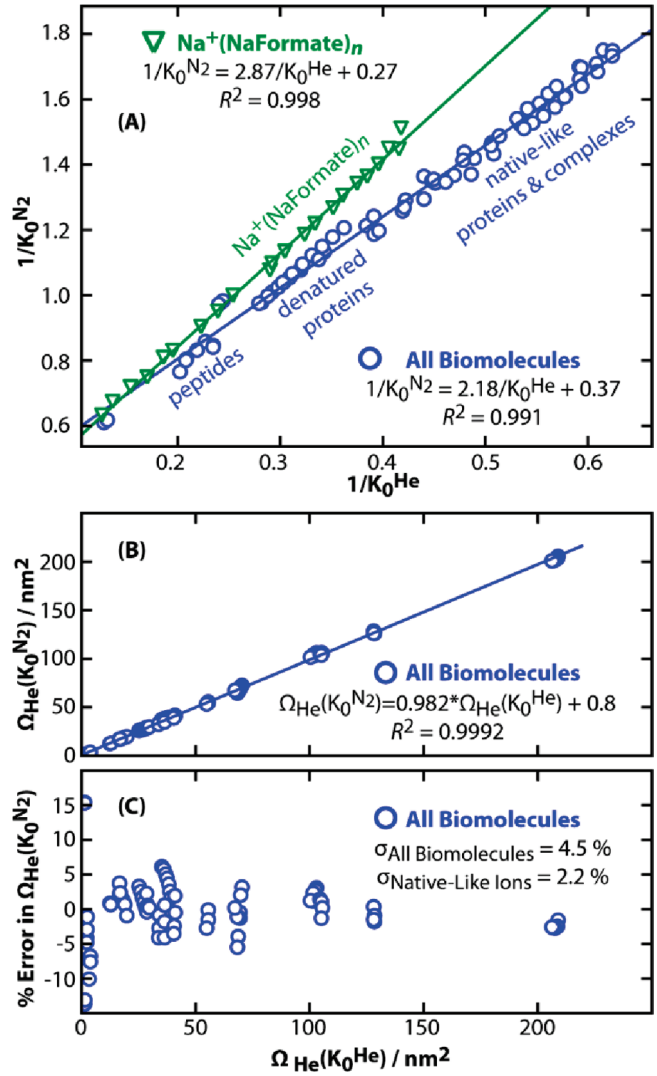

Figure 3. (A) Correlation between reciprocal reduced mobilities in helium and nitrogen drift gas. Values for biomolecular ions exhibit a linear relationship, as do preliminary values for $Na^+(NaFormate)_n$ (mobilities in each gas based on single drift time versus reciprocal drift voltage plots). (B) Collision cross sections in helium gas estimated from mobilities measured in nitrogen gas [$\Omega_{He}(K_0^{N_2})$], which were corrected using the relationship for biomolecules determined in part A, are well-correlated with those determined directly using mobilities measured in helium [$\Omega_{He}(K_0^{He})$]. (C) Standard deviation between $\Omega_{He}(K_0^{N_2})$ and $\Omega_{He}(K_0^{He})$ values is 4.5% for all ions, whereas that for just the native-like ions is only 2.2%.

A plot of reciprocal mobilities in helium ($1/K_0^{He}$) and nitrogen ($1/K_0^{N_2}$) gases shows that these values are well-correlated for the biomolecular ions investigated (Figure 3A). The relationship between these two quantities provides a means to convert $K_0^{N_2}$ values to effective K_0^{He} values, which in turn can be used to generate effective Ω_{He} values [$\Omega_{He}(K_0^{N_2})$] using eq 7. $\Omega_{He}(K_0^{N_2})$ values obtained using this approach are very close to $\Omega_{He}(K_0^{He})$ values over a wide range of Ω (Figure 3B). The relative errors of this approach can be substantial for the denatured peptides studied (up to 15%), but decrease substantially with increasing Ω (Figure 3C). For ions generated under native-like conditions, the relative errors are small (standard deviation = 2.2%). The relation-

(37) Kaddis, C. S.; Lomeli, S. H.; Yin, S.; Berhane, B.; Apostol, M. I.; Kickhoefer, V. A.; Rome, L. H.; Loo, J. A. *J. Am. Soc. Mass Spectrom.* **2007**, *18*, 1206–1216.
(38) Tammet, H. *J. Aerosol Sci.* **1995**, *26*, 459–475.
(39) Fischer, H.; Polikarpov, I.; Craievich, A. F. *Protein Sci.* **2004**, *13*, 2825–2828, and references therein.
(40) Quillin, M. L.; Matthews, B. W. *Acta Crystallogr.* **2000**, *D56*, 791–794.
(41) Ruotolo, B. T.; McLean, J. A.; Gillig, K. J.; Russell, D. H. *J. Mass Spectrom.* **2004**, *39*, 361–367.

ship between $1/K_0^{He}$ and $1/K_0^{N_2}$ appears quite stable; reoptimizing the relationship between $K_0^{N_2}$ and K_0^{He} (as carried out for the much large data set in Figure 3A) using data for only the native-like ions only reduces the relative errors to 2.1% (not shown). Therefore, errors between $\Omega_{He}(K_0^{N_2})$ and $\Omega_{He}(K_0^{He})$ for the ions generated under native-like conditions are small and similar to the associated errors in $K_0^{N_2}$ and K_0^{He}.

The relationship between $1/K_0^{He}$ and $1/K_0^{N_2}$ for multiply charged biomolecular ions does not appear to hold for all ions; this relationship for a set of sodium formate cluster ions ($Na^+[NaFormate]_n$) ions is significantly different from the relationship observed for biomolecular ions, even though the sodium formate cluster ions have similar ranges of mobilities as the biomolecular ions (Figure 3A). This indicates that determining $\Omega_{He}(K_0^{N_2})$ values for biomolecular ions using calibration with nonbiomolecular ions can induce significant errors, even if the biomolecular ions have mobilities that are similar to those of the nonbiomolecular ions. Although the precise mechanism underlying this observation is still under investigation, we speculate that the differences highlighted in Figure 3A might be attributable to polarization effects based on the relative availability of charges within the sodium formate cluster ions as compared to protection of charged groups in most biomolecular ions. Furthermore, such specific ion/drift-gas effects are likely to be more prevalent with decreasing Ω, as observed in our data. Such effects might be useful for increasing the specificity of ion identifications based on multiple mobility measurements made in different drift gases.

Calibration of Traveling-Wave Ion Mobility Drift Times. Ω values in traveling-wave ion mobility experiments are not determined directly from measured drift times, as is done for the RF-confining drift tube used in the experiments reported above, but are instead determined by calibrating drift times for ions of interest against those measured for ions of known Ω values. Calibration is necessary because the relationship between traveling-wave drift time and mobility is nonlinear, and the specific nonlinear factors that relate the two quantities depend strongly on experimental conditions and are difficult to determine a priori.[13−15,21] Calibration approaches for converting between IM drift times and Ω predate traveling-wave technologies,[42] and carry a number of advantages over direct Ω measurements. As in the case of modern mass spectrometry measurements, calibration enables measurements of high accuracy without detailed knowledge of instrument conditions (i.e., temperature, drift-gas pressure, drift-gas composition, and behavior). Consequently, calibration has the potential to enable robust and accurate Ω measurements that can be reproduced readily by different laboratories, providing a common frame of reference for all measurements.

To evaluate the effects of calibrant ion selection on the accuracy of the calibration, drift times for denatured peptide, denatured protein, and native-like protein complex ions were measured using a standard Synapt G1 HDMS instrument with a traveling-wave ion mobility cell. Experiments were performed in 0.4 Torr N_2 at three wave heights (8, 9, and 10 V) and constant wave velocity (300 m/s). Numerous protocols have been reported for calibrating traveling-wave ion mobility drift times.[13−15] For the analysis below, we used a modified form of a protocol reported previously (vide supra).[13] Note that the use of an exponential factor in this protocol to correct the drift times prior to the creation of a linear calibration plot is analogous to the use of a power function to create a nonlinear calibration plot, as used in some alternative calibration protocols.[14,15]

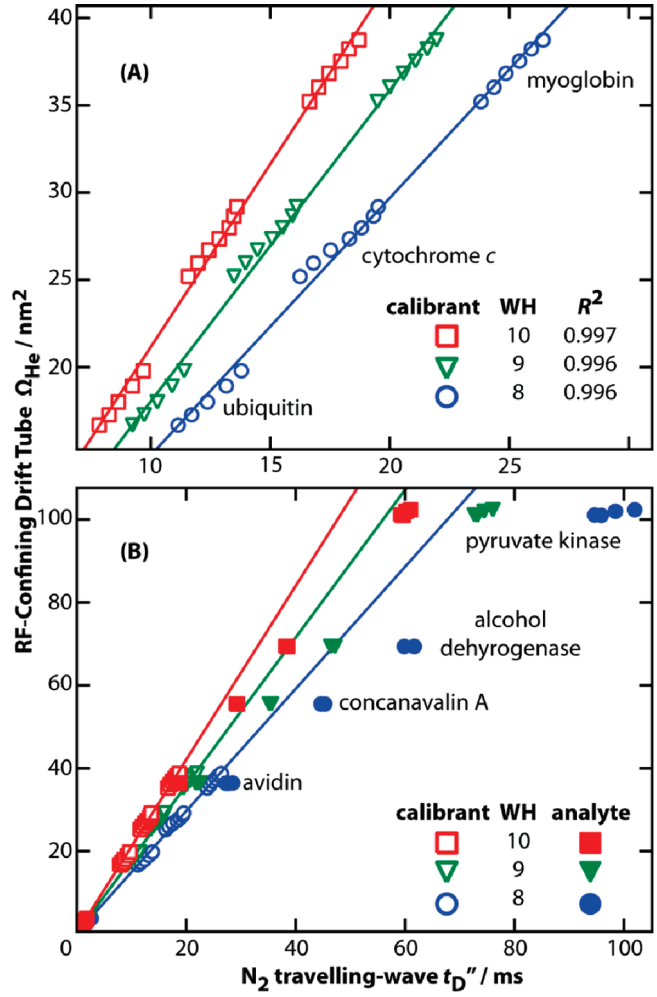

Figure 4. (B) Calibrating traveling-wave drift times using only denatured ubiquitin, cytochrome *c*, and myoglobin ions. (A) Expansion of data for denatured protein ions. Traveling-wave drift times were measured using 0.4 Torr N_2; a wave velocity of 300 m/s; and wave heights (WHs) of 8 V (red squares), 9 V (green triangles), or 10 V (blue circles). Data used to obtain the exponential factor are represented with hollow markers (A and B), whereas all other data are represented with solid markers (B).

Most reported Ω_{He} values for protein complexes have been based on calibrations using denatured monomeric proteins,[7,15,22,23] typically ubiquitin, cytochrome *c*, and myoglobin. To evaluate the effects of such a calibration, the traveling-wave data described above were calibrated using only results for denatured ubiquitin, cytochrome *c*, and myoglobin (Figure 4). Data used to obtain the calibration functions are well-correlated with those respective calibration functions (Figure 4A). Calibrated Ω_{He} values for native-like protein complexes, however, exhibit increasingly large errors with increasing mass (Figure 4B); for example, denatured protein ions are less effective for calibration of larger native-like ions than the smaller native-like ions investigated. Using these calibrations at 8, 9, and 10 V wave heights would result in protein complex Ω_{He} values that are 11−47%, 7−33%, and 5−25% larger,

(42) Ruotolo, B. T.; Russell, D. H. *J. Phys. Chem. B* **2004**, *108*, 15321–15331.

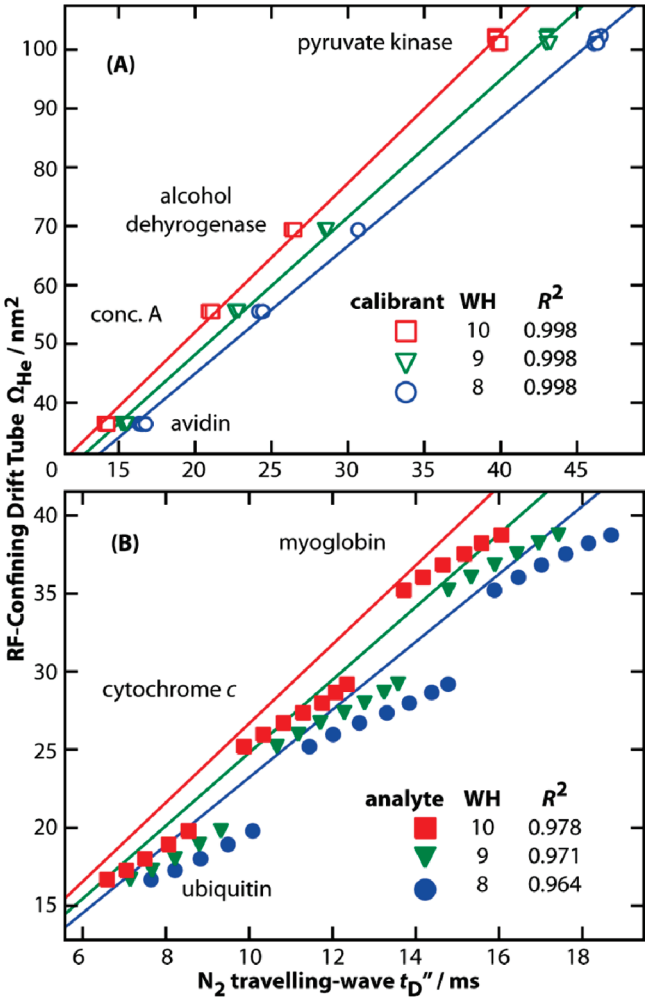

Figure 5. (A) Calibrating traveling-wave drift times using only native-like protein complex ions. Traveling-wave drift times were measured using 0.4 Torr N_2; a wave velocity of 300 m/s; and wave heights (WHs) of 8 V (red squares), 9 V (green triangles), or 10 V (blue circles). (B) Expansion of data for denatured protein ions. Correlation coefficients in B are for the correlation between the data for the denatured protein ions and the calibration plot obtained using only data for native-like protein complex ions.

respectively, than those measured directly using the RF-confining drift tube.

Recently, both protein complex and denatured monomeric protein ions have been used to calibrate traveling-wave drift times for protein complexes of interest.[5] To evaluate the effects of this calibration scheme, the same traveling-wave data as used for Figure 4 were recalibrated using all denatured protein and native-like protein complex ions investigated (Figure S2, Supporting Information). The experimental data are well-correlated with their respective calibration functions ($R^2 \geq 0.998$), and the calibrated Ω_{He} values obtained for protein complex ions using traveling-wave drift times are indistinguishable [$(-1.2 \pm 1.9)\%$] from the direct Ω_{He} values obtained using the RF-confining drift tube.

The same traveling-wave data were also calibrated using only protein complex ions (Figure 5A). Data used to optimize the calibration functions are well-correlated with those respective calibration functions ($R^2 \geq 0.998$), and the three wave heights used here yield protein complex Ω values that are very similar, $+(0.2 \pm 1.9)\%$, to those measured directly using the RF-confining drift tube. Significantly, there is no systematic deviation between the direct and indirect Ω values, and the random deviation is comparable to the uncertainties in the direct measurements.

Ω_{He} values for protein complex ions obtained through calibration using both denatured protein and protein complex ions (Figure S2, Supporting Information) or only protein complex ions (Figure 5A) appear to be essentially independent of the wave height selected, whereas those obtained through calibration using only denatured protein ions (Figure 4B) depend strongly on the wave height selected. The calibration protocol used here[13] dictates rejecting calibrated Ω values that depend strongly on wave height (such as Figure 4) to limit field-dependent influences on calibrated Ω values.[13] These results suggest that this control might also limit extrapolation errors when protein complex ions have very different mobilities than the calibrant ions, as described here. Therefore, it is likely that Ω values based on traveling-wave drift times and calibration using denatured proteins that followed correctly the previous protocol[13] might have errors that are at the lower end of the ranges suggested by the results from Figure 4.

The calibration plots shown in Figures 4 and 5, as well as Figure S2 of the Supporting Information, did not use the traveling-wave data for a small set of denatured peptide ions to determine the exponential factor. In all cases, analogous calibration plots that also used data for the denatured peptide ions to determine the exponential factor resulted in poorer fits for native-like protein complex ions. This suggests that there might be additional higher-ordered effects that are increasingly significant when comparing ions of increasingly different masses and mobilities. Therefore, using calibrant ions that have masses and mobilities most similar to those of the analyte ions is likely to result in smaller errors than using calibrant ions with broad ranges of masses and mobilities.

Using native-like protein complex ions to obtain the calibration plots results in more accurate Ω values for native-like protein complex ions and less sensitivity to the specific traveling-wave conditions used. The systematic error when calibrating with both denatured protein and native-like protein complex ions (1.2%) is larger than that when calibrating with only native-like protein complex ions (0.2%), although both of these values are small relative to the uncertainties in those quantities (1.9% for each). Calibration using both denatured protein and native-like protein complex ions (Figure S2B, Supporting Information) or only native-like protein complex ions (Figure 5B) results in poorer correlation coefficients for the denatured protein ions than that obtained when calibrating using only denatured protein ions (Figure 4A) In Figures S2B (Supporting Information) and 5B, data for each denatured protein are skewed relative to the respective calibration function, features that are also present in a previously reported calibration plot that used both denatured protein and native-like protein complex ions.[5] These results indicate that calibration will yield the most accurate Ω values when drift times for ions of interest are corrected using an exponential factor determined for a set of ions with similar properties. For native-like protein complex ions, the addition of denatured protein ions to a calibration set containing adequate native-like protein complex ions

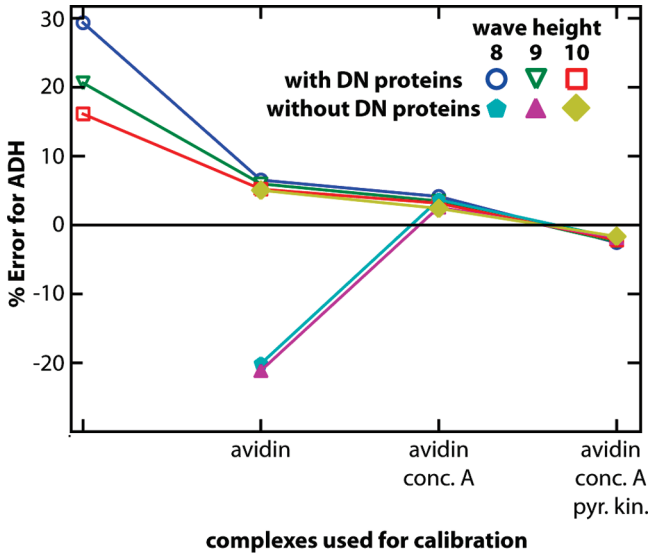

Figure 6. Effect of calibrant ion selection on the calibrated collision cross section (Ω_{He}^{Cal}) of alcohol dehyrdogenase (ADH). Ω_{He}^{Cal} was determined using a series of calibration sets, both with and without denatured (DN) proteins, and with an increasingly large set of native-like protein complex ions. The addition of native-like protein complexes reduces the deviation from values measured directly using the RF-confining drift tube (Ω_{He}^{Dir}). The percentage error was determined as $(\Omega_{He}^{Cal} - \Omega_{He}^{Dir})/\Omega_{He}^{Dir}$ for ADH.

will result in negligible or even detrimental affects to the accuracy of the calibrated Ω values.

Effects of Calibrant Ion Selection for Native-Like Alcohol Dehydrogenase (ADH) Ions. To characterize the effects of calibrant ion selection for determining Ω values for specific ions, a series of calibration schemes were used to determine the Ω values for native-like ADH ions, using the same traveling-wave drift time data as shown in Figures 4, 5, and S2 (Supporting Information). The results are summarized in Figure 6 by plotting the relative difference between the calibrated (Ω_{He}^{Cal}) and direct (Ω_{He}^{Dir}) values for the two observed charge states that are also included in Table S3 (Supporting Information). First, data for native-like protein complex ions are sequentially added to data for the denatured protein ions (hollow markers) and then used to calibrate traveling-wave drift times for the ADH ions. Calibration using only denatured protein ions (left-most data, equivalent to the results shown in Figure 4B) results in significant errors for ADH (Ω_{He}^{Cal} values are 16%, 21%, and 29% greater than Ω_{He}^{Dir} values at wave heights of 8, 9, and 10 V, respectively) that depend strongly on mobility conditions. Adding one (avidin, +5.9% relative error), two (avidin and concanavalin A, +3.6%), or three protein complexes (avidin, concanavalin A, and pyruvate kinase, −2.4%) to the calibration set significantly reduces both the average relative errors and the wave-height-dependent effects.

Increasingly large data sets containing only native-like protein complex ions (solid markers) were also used to calibrate traveling-wave drift times for ADH ions. Calibration using only avidin and no denatured protein ions results in Ω_{He}^{Cal} values for ADH that are −20%, −21%, and +5% different from those for Ω_{He}^{Dir}, but these results were not expected to be particularly accurate because of the inherent limitations of generating a nonlinear calibration plot using only three calibrant ion drift times (three charge states observed for avidin). Calibration using multiple protein complexes results in significantly reduced relative errors and stable Ω_{He}^{Cal} values: Calibration using avidin and concanavalin A results in Ω_{He}^{Cal} values for ADH that are 2.9% greater than the corresponding Ω_{He}^{Dir} values; and calibration using avidin, concanavalin A, and pyruvate kinase results in Ω_{He}^{Cal} values that are 1.8% smaller than the corresponding Ω_{He}^{Dir} values. Interestingly, if only concanavalin A and pyruvate kinase ions are used to obtain the calibration plot, Ω_{He}^{Cal} values that are only 0.7% less than the corresponding Ω_{He}^{Dir} values are obtained (not shown in figure), indicating that very small errors can be achieved using a small number of calibrant ions so long as they closely bracket the masses and mobilities of the analyte ions of interest.

CONCLUSIONS

The recent availability of traveling-wave ion mobility hybrid mass spectrometers has enabled the rapid adoption of ion mobility techniques by a large and rapidly growing community. This work provides a detailed framework for assessing and reducing the errors associated with using traveling-wave drift times for determining absolute Ω values for ions spanning masses and Ω values differing by more than 2 orders of magnitude.

These and other efforts by the authors to calibrate traveling-wave drift times for protein complexes on other Synapt G1 HDMS and Synapt G2 HDMS instruments indicate that small calibration errors are readily achieved when using at least two native-like IM standards that closely bracket the masses and mobilities of the analyte ion of interest. Closely bracketing the native-like ion is preferable to using a larger set of IM standards with a broad range of mobilities and masses. This is due to the fact that the use of closely bracketed calibrant ions mitigates the need to characterize further ion transport properties in the instrument, which results in smaller extrapolation errors. Errors for the calibrated Ω values will include contributions from the uncertainties of Ω values for the calibrant ions (3% for the values reported in Tables S2 and S3, Supporting Information), the reproducibility of the drift times measured for the calibrant and analyte ions, and other factors. These results and other experiments in our laboratories indicate that careful experimental design and execution can result in calibrated Ω values with propagated errors of less than 5%.

Measuring collision cross sections using traveling-wave ion mobility spectrometry and this new calibration framework offers many advantages. Measuring drift times for calibrant and analyte ions under the same experimental conditions removes the need for accurate knowledge of drift-gas temperature, composition, and pressure, as well as cell geometry. All of these parameters are critical for determining Ω values directly from drift tube measurements. This calibration framework enables different laboratories to produce consistent Ω measurements and develop universal tools for interpreting those results. Ultimately, this enables the generation of better structural constraints from IM experiments, which will result in the generation of more accurate three-dimensional models of protein and other biomolecular complexes.

The Ω database also provides a foundation for understanding the general relationship between gas-phase and condensed-phase structures for native-like protein and protein complex ions. This

is important for determining how IM-MS results should be used to constrain models for condensed-phase structures. For example, the average effective density for the ions in Table S3 (Supporting Information) is 0.6 g cm^{-3}, which is similar to the value based on GEMMA experiments[37] and significantly less than values for the solvent-excluded regions of proteins proteins.[43] This suggests that these ions have significant memory of their solution-phase structure and have not collapsed to form globular structures. More generally, the database values provide valuable benchmarks for computational approaches for estimating Ω values for models and, in particular, for developing strategies for estimating Ω_{N_2} values, which are not well-described in the literature. Finally, these values can be used to develop a more detailed understanding of the effects of charge state on Ω values and noncorrelated differences between Ω_{He} and Ω_{N_2}, which will likely be important for further refinement of ion mobility constraints in the gas-phase structural biology process.

(43) Liang, J.; Dill, K. A. *Biophys. J.* **2001**, *81*, 751–766.

ACKNOWLEDGMENT

M.F.B. is a Waters Research Fellow, and C.V.R. is a Royal Society Research Professor.

SUPPORTING INFORMATION AVAILABLE

Method for calculating effective densities, Tables S1−S3, and Figures S1 and S2. This material is available free of charge via the Internet at http://pubs.acs.org.

Received for review September 2, 2010. Accepted October 8, 2010.

AC1022953